Computer Modeling for Assessing the Detectability of the Transition Zone in the Basement Complex Terrain of Southwest Nigeria.

Lawrence O. Ademilua, Ph.D.[1*] and Martins O. Olorunfemi, Ph.D.[2]

[1]Department of Geology, University of Ado-Ekiti, Nigeria.
[2]Department of Geology, Obafemi Awolowo University, Ile-Ife, Nigeria.

E-mail: adeoladimeji@yahoo.com*
mlorunfe@yahoo.co.uk

ABSTRACT

The main objective of this research is to theoretically model a basement profile containing the transition zone with varying thicknesses and resistivities as a means of assessing the detect ability of the zone. This is because the zone has the tendency to be suppressed on the Vertical Electrical Soundind (VES) curve due to its intermediate resistivity and often thin thickness. The research approach has been to use a forward modeling computer software (BABRES 1.0) developed for that purpose by the authors, for generating theoretical Schlumberger VES curves for typical basement complex profiles containing the transition zone while varying its thicknesses and resistivities. From the series of four-layer HA-type and five-layer KHA-type model curves generated by variously keeping the resistivities of the topsoil, weathered layer, transition zone and basement bedrock constant and varying the thickness of the transition zone between 2m and 50m, it was observed that the transition zone becomes detectable with a thickness ratio greater than or equal to 0.73 for HA-and 1.11 for the KHA-type curves, while the resistivity ratios permitting detectability range between 1.67 to 3.67 for the HA-type, and 1.67 to 4.33 for the KHA-type curves. Below these ranges the zone becomes undetectable.

(Keywords: computer modeling, VES, BABRES, basement complex profiles)

INTRODUCTION

One of the subsurface horizons with tendency to be suppressed on the Vertical Electrical Sounding (VES) curve is the transition zone between the weathered basement (saprolite) layer and the underlying fresh basement (Figure 1).

Suppression results when the thickness of the layer is very small compared to its depth (its resistivity is neither zero nor infinity). The effect of such a layer on the apparent resistivity curve is negligible and its presence 'suppressed' (Parasnis, 1994). One of the important problems in the interpretation of vertical sounding for multi-layer earth models is electrical suppression which implies that when a deeply buried layer is appreciably thin, its effect on the sounding curve may be negligible (Maillet, 1947; Flathe, 1963; Kunetz, 1966). A typical geological situation in which suppression is encountered is in the identification of fractured bedrock in areas underlain by crystalline basement complex rocks. (Olayinka and Oladipo, 1994).

The factors influencing geoelectrical suppression of layers on the VES curve include amongst others, thickness, resistivity and reflection coefficient of between succeeding layers (Olayinka and Oladipo, 1994). The weathered profile consists of a highly resistive top-soil layer, a relatively low resistivity regolith comprising a mixture of clay and sand materials, and fresh bedrock whose resistivity is so high as to be considered infinite for all practical purposes (Figure 1). The generalized or model sounding curve in the area is of the type $\rho_1 > \rho_2 < \rho_3$ (H-type).Generally, to interprete Schlumberger VES data, the measured apparent resistivity data are plotted against electrode spacing on transparent bi-log graph sheet to produce a sounding curve which is now placed on master curves and appropriately adjusted until a perfect or interpolated match is obtained and subsequent layer parameters deduced.

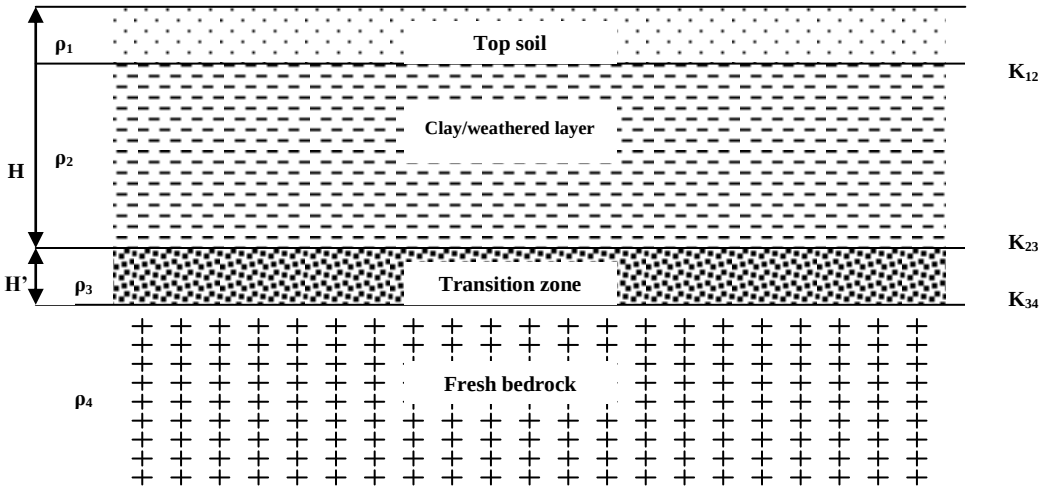

Figure 1: Model of a Typical 4-layer Earth in the Basement Complex Showing the Transition Zone.

The layer parameters (layer resistivities and thicknesses) obtained are fed into the computer and used to generate theoretical curves for comparison with field data generated curve and the degree of fitness or similarities calculated to obtain the error levels between the starting and the final model parameters (Mooney and Orellana, 1966).

However, one of the important sources of non-uniqueness in the interpretation of VES data for multi-layer earth models is electrical suppression which in practical terms implies that unless a deeply buried layer is appreciably thick, its effect on the sounding curve may be negligible. When a layer is suppressed, it becomes very difficult to detect its signature on the VES curve, thus giving an impression of its non–existence and hence missing from interpretation considerations. The tendency, for example, is to misinterpret a four-layer HA curve for a three–layer H curve (Olayinka and Oladipo, 1994).

In some cases however, there is a partly weathered/fractured basement between the weathered layer and the fresh bedrock. The resistivity of this layer is intermediate between those of the overlying and underlying beds. The generalized sounding curve in this case is of the type $\rho_1 > \rho_2 < \rho_3 < \rho_4$ (HA). However the field situation in which the effect of this layer on the resultant vertical sounding curve may not be appreciable is called suppression. Here the four layer HA-type curve is inadvertently interpreted as a three layer H-type curve thereby resulting in a serious interpretation error which equally affects all subsequent decisions taken on it.

The interpretation and modeling of electrical resistivity field data are commonly done by assuming that the subsurface consists of a system of uniform and homogeneous parallel layers (Irshad, 1976). Quite commonly, the non-uniqueness of the interpretation from areas underlain directly by crystalline basement rocks is always expressed in terms of the ability to reliably estimate the depth to bedrock and possibly detect the transition zone below the saprolite (Hazel, et al., 1988; Barker, 1992; Carruthers and Smith, 1992). The transition zone as earlier discussed is that zone of relatively much lower resistivity than the underlying fresh bedrock (Figure 1). It must be noted however that this zone is not generally observable in all locations in the basement complex.

RESEARCH METHODOLOGY

The typical resistivity sounding curves depicting the location of the transition zone plus the overlying weathered layer is the HA- or KHA-type curve (Figure 2).

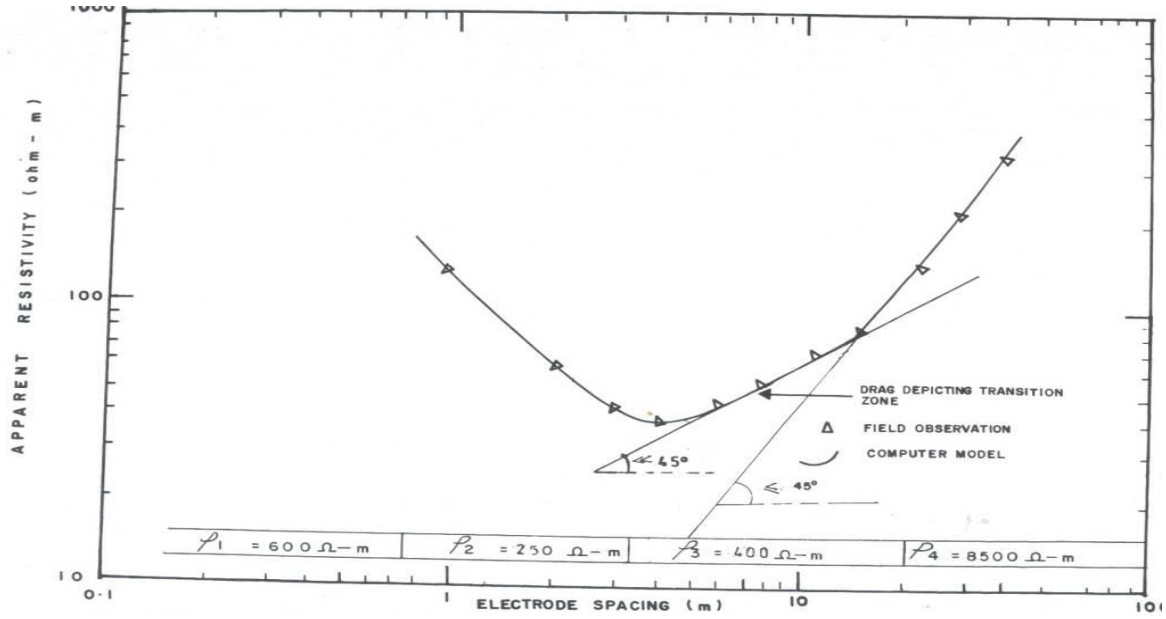

Figure 2: Geoelectric Signatures of a Basement Complex Profile Containing the Transition Zone.

This curve is usually characterized by a gentle drag along the rising (basement) segment. While a somewhat undefined infinite resistivity value may be assigned to the supposedly fresh massive, compact and unfractured rock, the value for fractured basement rocks is often less than 1000 ohm-m (Beeson and Jones, 1988; David, 1988; Olayinka, 1996; Olorunfemi et al., 2005).

The resistivity of the transition zone is usually intermediate between those of the overlying weathered and underlying fresh bedrock. However, the thickness of the zone must be appreciable for its impact to be noticeable on the VES curve, failing which it might be suppressed and its signature or effect unresolved and undetected, thereby leading to a typical four-layer curve being misinterpreted as a three-layer curve.

Zohdy et al., (1974), indicated that the detectability of a buried layer depends on its relative thickness, i.e. ratio of the bed thickness to its depth of burial. Also Verma et al., (1988), in particular, emphasized that for vertical electrical sounding to be successful, the target should have a relative thickness exceeding 1.0 while Parasnis, (1986) introduced another condition that the resistivity of the target should neither be infinite nor zero.

To attempt to resolve the detectability question therefore, a forward Modelling Software BABRES 1.0 ((Ademilua, (2007); Ademilua and Olorunfemi, (2007)) developed by this author for the purpose was used to facilitate the generation of series of four-layer HA- and five-layer KHA- type model curves depicting the situation. In doing this, two approaches were adopted.

In the first approach, for fixed values of the resistivities and thicknesses of the other three layers (for HA-type curves), the thickness of the transition zone was varied in step of 2 m between 2 m and 56 m for a given transition zone resistivity. This is in agreement with Acworth, (1987); Buckley and Zeil, 1984; White, et al., 1988; Olayinka and Oladipo (1994) as they all posited that in crystalline basement areas, the thickness of the weathered zone is commonly less than 30 m while the thickness of the topsoil layer hardly exceeds about 2 m. Therefore, the thickness of the topsoil was fixed at 1m, that of the weathered layer was put at 10m, while the transition zone's thickness was put at 2 m for the starting model. The layer resistivity values were fixed at 500 ohm-m, 150ohm-m, 300ohm-m, and 10,00ohm-m, respectively.

This procedure was also followed in the case of the case of the KHA-type curves except that the thickness of the transition zone was varied in steps of 5m, between 5m and 80m, for a given transition zone resistivity, while the layer resistivity values were fixed at 200 ohm-m, 750 ohm-m,150 ohm-m,250 ohm-m and 10000ohm-m respectively for the horizons.

For each of the resulting parameter set from the variations, a model curve was generated using the developed software (BABRES 1.0). The curves generated include 27 Models (A1-A27) for the HA-type, and 17 Models (J1-J17) for the KHA-type curves (see Figures 3-7 for representative models of the HA-type, and Figures 8-11 for the KHA-type curves) were thereafter carefully examined for the signatures of the transition zone. Where this is detectable, the drag lengths (in cm) which is the linear extent of the transition zone as detected within the rising segment of the curve were measured, so also was the drag angle β^{o} which a tangential line drawn at the drag surface makes with the horizontal axis measured and recorded (see Tables 1 and 2, respectively for the summary of the resulting parameter sets and the obtained/measured specifications of the detectable transition zones for the HA- and KHA-type curves).

In the second approach and for the HA-type curves, the resistivities of the other three layers were fixed while that of the transition zone was varied. The resistivity was varied from 250 ohm-m to 850 ohm-m for the transition zone. For the starting model, the resistivities are 500 ohm-m for topsoil, 150 ohm-m for weathered layer, 250 ohm-m for the transition zone while the fresh basement has a resistivity of 10000 ohm-m.

The thicknesses of the starting models are 1 m for topsoil, 10 m for weathered layer while the transition zone has a thickness of 2 m. Each of the resulting parameter sets was used to generate seven (7) model curves numbered B1-B7, C1-C7, D1-D7, E1-E7, F1-F7, G1-G7,H1-H7 for the HA- type curves, (see Figures 12-18 for representative sample models generated for the HA- type curve).

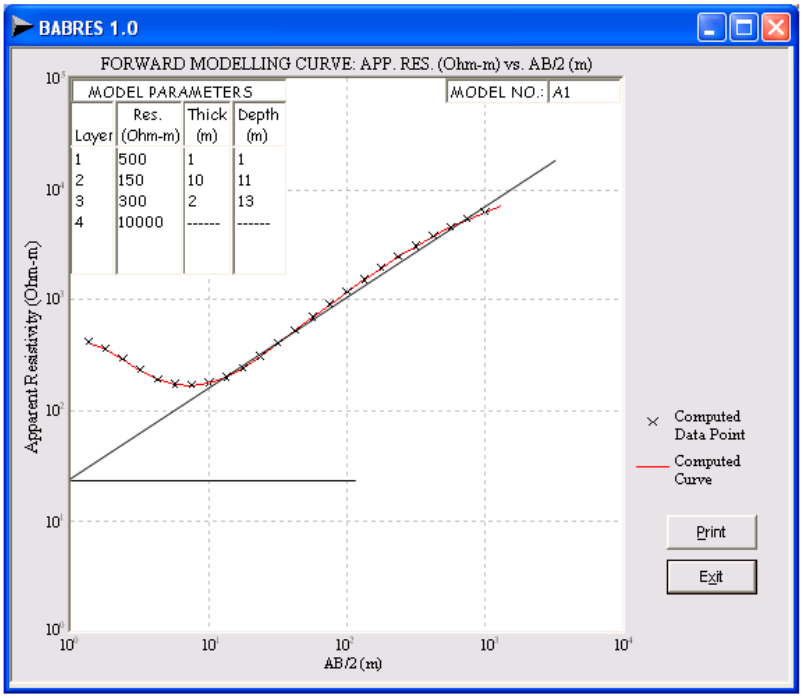

Zone not detectable, drag angle β = 0°

Figure 3: HA-Type Curve Model A1 for Thickness of Transition Zone Equals 2m.

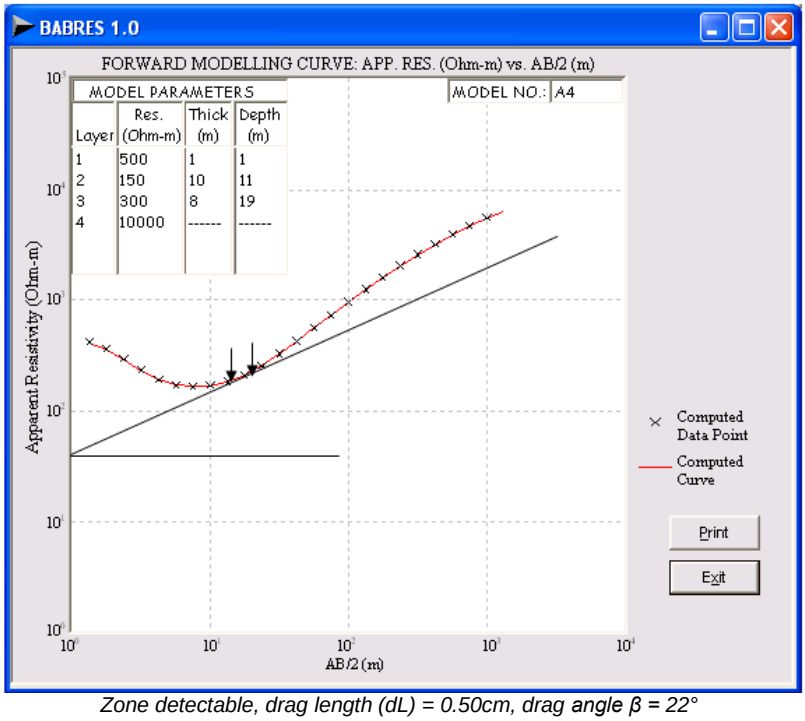

Zone detectable, drag length (dL) = 0.50cm, drag angle β = 22°

Figure 4: HA-Type Curve Model A4 for Thickness of Transition Zone Equals 8m.

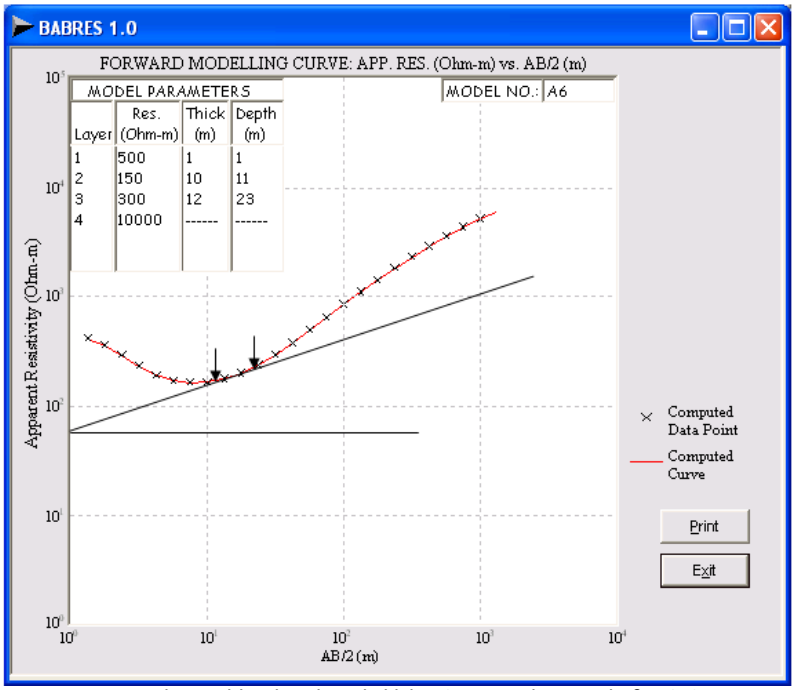

Zone detectable, drag length (dL) = 0.75cm, drag angle β = 21°

Figure 5: HA-Type Curve Model A6 for Thickness of Transition Zone Equals 12m.

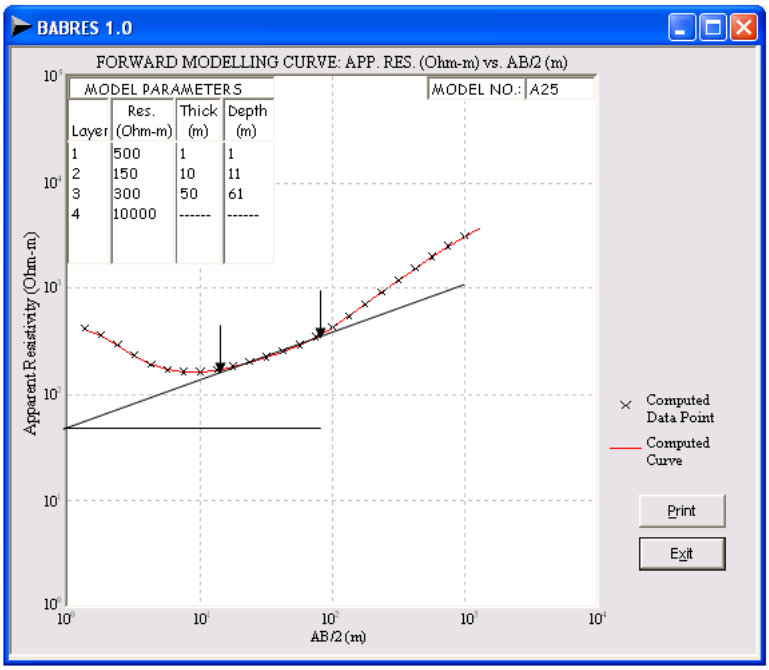

Zone detectable, drag length (dL) = 2.5cm, drag angle β = 21°

Figure 6: HA-Type Curve Model A25 for Thickness of Transition Zone Equals 50m.

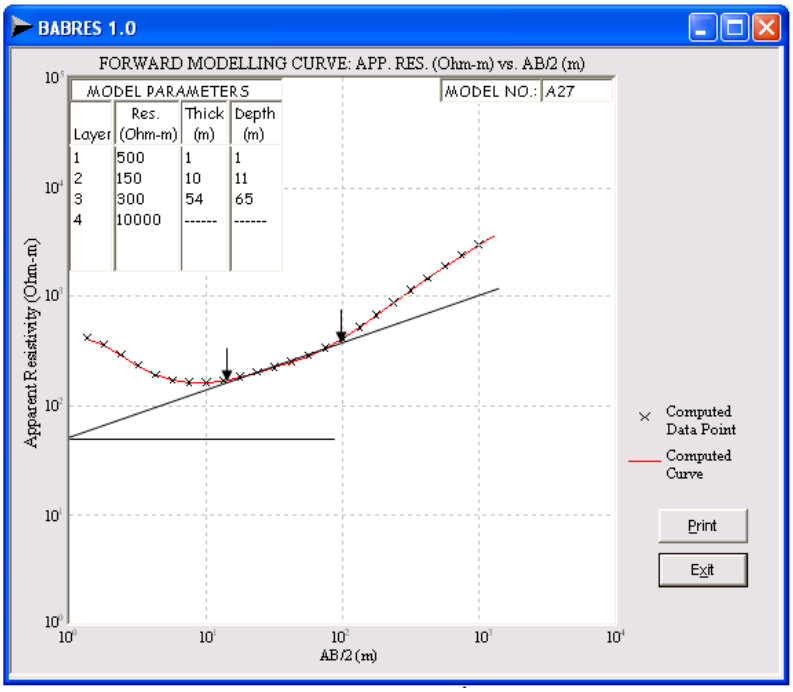

Zone detectable, drag length (dL) = 2.6cm, drag angle β = 22°

Figure 7: HA-Type Curve Model A27 for Thickness of Transition Zone Equals 54m.

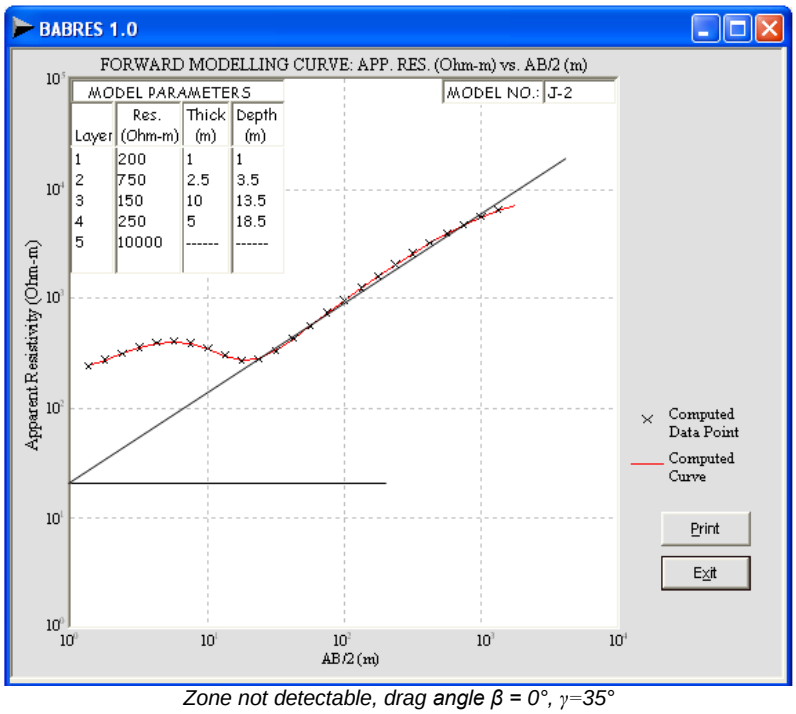

Zone not detectable, drag angle β = 0°, γ=35°

Figure 8: KHA-Type Curve Model J-2 for Thickness of Transition Zone Equals 5m.

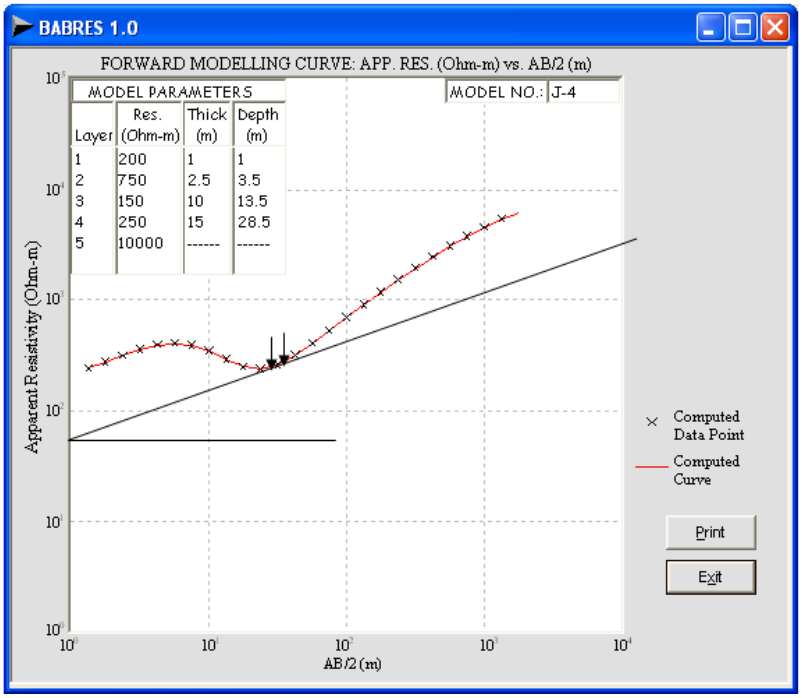

Zone detectable, drag length (dL) 0.20cm, drag angle β = 21°

Figure 9: KHA-Type Curve Model J-4 for Thickness of Transition Zone Equals 15m.

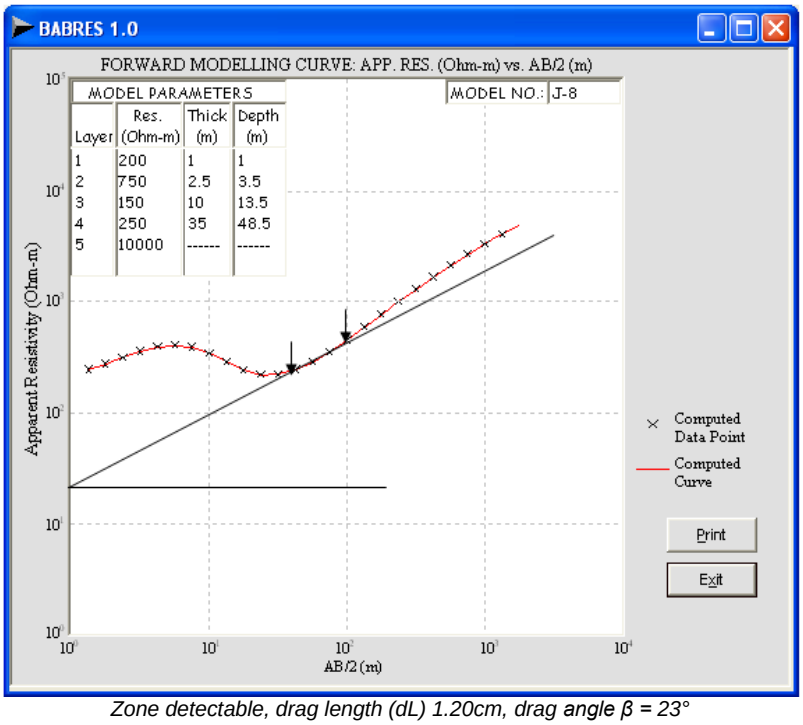

Zone detectable, drag length (dL) 1.20cm, drag angle β = 23°

Figure 10: KHA-Type Curve Model J-8 for Thickness of Transition Zone Equals 35m.

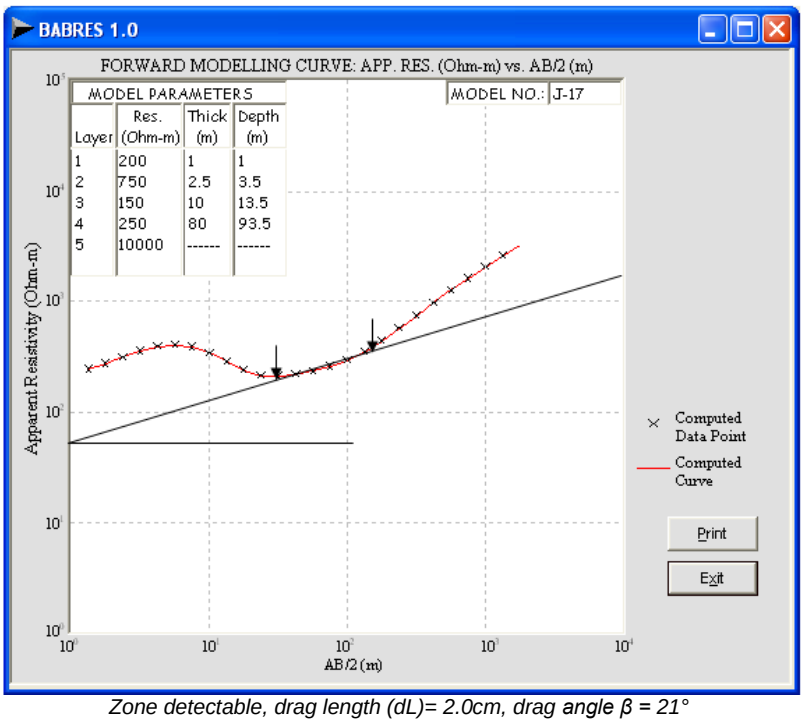

Zone detectable, drag length (dL)= 2.0cm, drag angle β = 21°

Figure 11: KHA-Type Curve Model J-17 for Thickness of Transition Zone Equals 80m.

Table 1A: Effect of Variation of Thickness of Transition Zone on the Detectability Parameters of the HA-Type VES Curve.

Layer No	MODELS A1 - A15 Thicknesses (m)															
1	500	1	1	1	1	1	1	1	1	1	1	1	1	1	1	1
2	150	10	10	10	10	10	10	10	10	10	10	10	10	10	10	10
3	300	2	4	6	8	10	12	`14	16	18	20	22	24	26	28	30
4	10000	-	-	-	-	-	-	-	-	-	-	-	-	-	-	-
	H	11	11	11	11	11	11	11	11	11	11	11	11	11	11	11
	H'	2	4	6	8	10	12	14	16	18	20	22	24	26	28	30
	H'/H	0.18	0.36	0.55	0.73	0.91	1.09	1.27	1.45	1.64	1.82	2.00	2.18	2.36	2.55	2.73
		0	0	0	22	22	21	19	19	22	20	20	20	20	21	21
	dL (cm)	0	0	0	0.50	0.70	0.70	0.70	0.80	1.3	1.35	1.40	1.60	1.60	1.80	1.90
	Remarks	ND	ND	ND	D	D	D	D	D	D	D	D	D	D	D	D

Table 1B: Effect of Variation of Thickness of Transition Zone on the Detectability Parameters of the HA-Type VES Curve.

Layer No	MODELS A16 – A27 Thicknesses 9m)													
1	500	1	1	1	1	1	1	1	1	1	1	1	1	
2	150	10	10	10	10	10	10	10	10	10	10	10	10	
3	300	32	34	36	38	40	42	`44	46	48	50	52	54	
4	10000	-	-	-	-	-	-	-	-	-	-	-	-	
	H	11	11	11	11	11	11	11	11	11	11	11	11	
	H'	32	34	36	38	40	42	44	46	48	50	52	54	
	H'/H	2.91	3.09	3.27	3.45	3/64	3.83	4.00	4.18	4.36	4.55	4.73	4.91	
		21	21	21	21	22	22	21	22	21	22	22	22	
	dL (cm)	2.0	2.0	2.2	2.2	2.3	2.4	2.4	2.4	2.5	2.5	2.5	2.6	
	Remarks	D	D	D	D	D	D	D	D	D	D	D	D	

Note: ND = Transition zone not detectable , D = Transition zone detectable , H = Thickness of the overlying layers , H' = Thickness of the transition zone , H'/H = Thickness ratio , dL = drag length , β = inclination angle of drag (transition zone) segment

Table 2A: Effect of Variation of Thickness of Transition Zone on the Detectability Parameters of the KHA-Type VES Curve.

Layer No	MODELS J1 - J17 Thicknesses (m)															
1	200	1	1	1	1	1	1	1	1	1	1	1	1	1	1	1
2	750	2.5	2.5	2.5	2.5	2.5	2.5	2.5	2.5	2.5	2.5	2.5	2.5	2.5	2.5	2.5
3	150	10	10	10	10	10	10	10	10	10	10	10	10	10	10	10
4	250	2	4	5	10	15	20	25	30	35	40	45	50	55	60	65
5	10000	-	-	-	-	-	-	-	-	-	-	-	-	-	-	-
	H	13.5	13.5	13.5	13.5	13.5	13.5	13.5	13.5	13.5	13.5	13.5	13.5	13.5	13.5	13.5
	H'	2	4	5	10	15	20	25	30	35	40	45	50	55	60	65
	H'/H	0.15	0.30	0.37	0.74	1.11	1.48	1.85	2.22	2.59	2.96	3.33	3.70	4.07	4.44	4.81
		0	0	0	0	22	21	23	23	23	23	23	23	23	22	22
	dL (cm)	0	0	0	0	0.20	0.30	0.45	0.60	1.20	1.30	1.35	1.35	1.50	1.50	1.70
	Remarks	ND	ND	ND	ND	D	D	D	D	D	D	D	D	D	D	D

Table 2B

Layer No	MODELS J16- J17 Thicknesses (m)		
1	200	1	1
2	750	2.5	2.5
3	150	10	10
4	250	70	75
5	10000	-	-
	H	13.5	13.5
	H'	70	75
	H'/H	5.19	5.55
		22	22
	dL (cm)	1.70	1.70
	Remarks	D	D

Note: ND = Transition zone not detectable , D = Transition zone detectable , H = Thickness of the overlying layers , H' = Thickness of the transition zone , H'/H = Thickness ratio , dL = drag length , β = inclination angle of drag (transition zone) segment

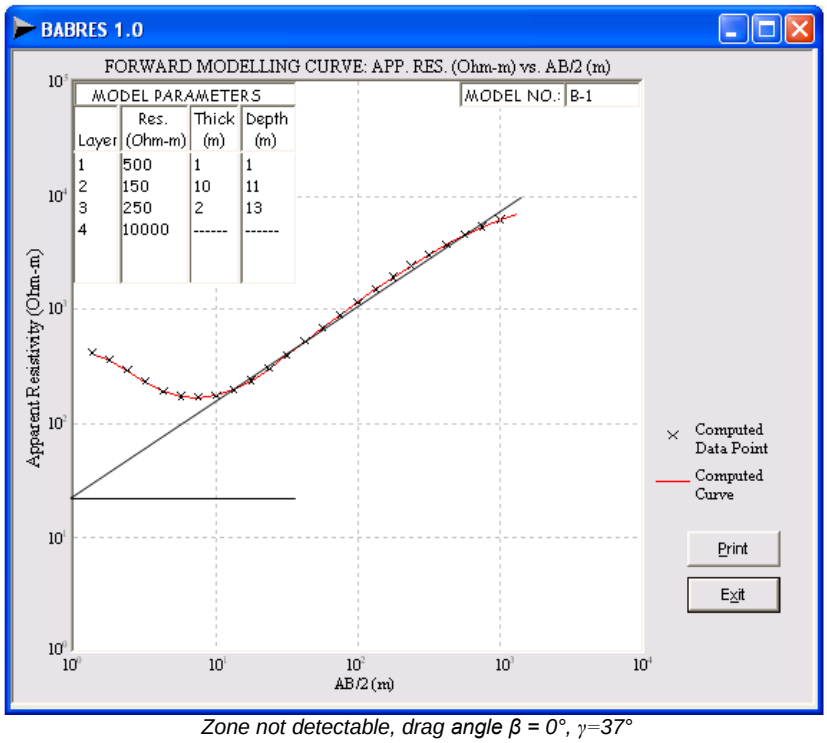

Zone not detectable, drag angle β = 0°, γ=37°

Figure 12: HA-Type Curve Model B1 for Resistivity of Transition Zone Equals 250 ohm-m.

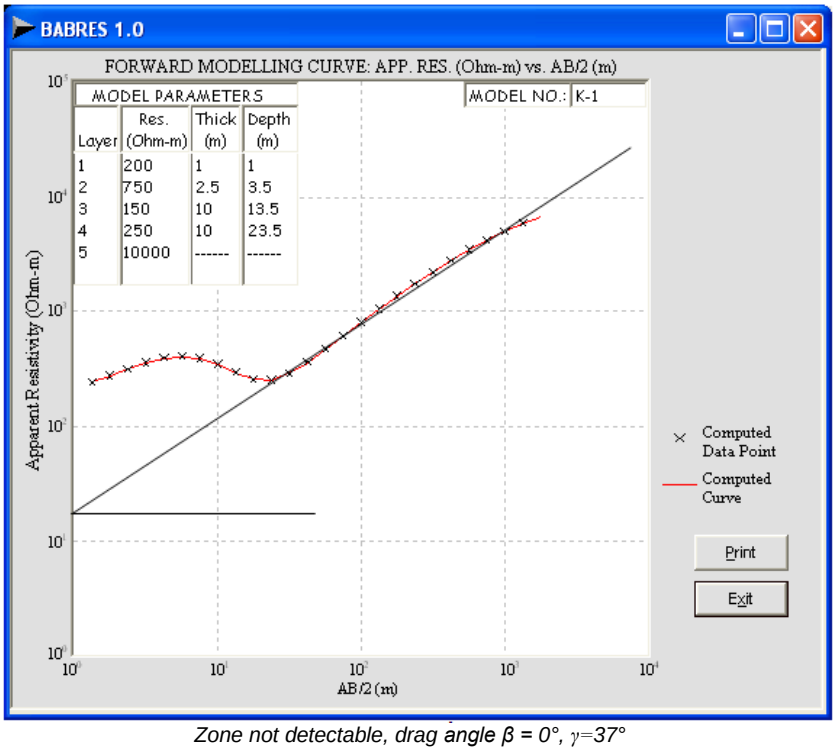

Zone not detectable, drag angle β = 0°, γ=37°

Figure 13: KHA-Type Curve Model K1 for Resistivity of Transition Zone Equals 250 ohm-m.

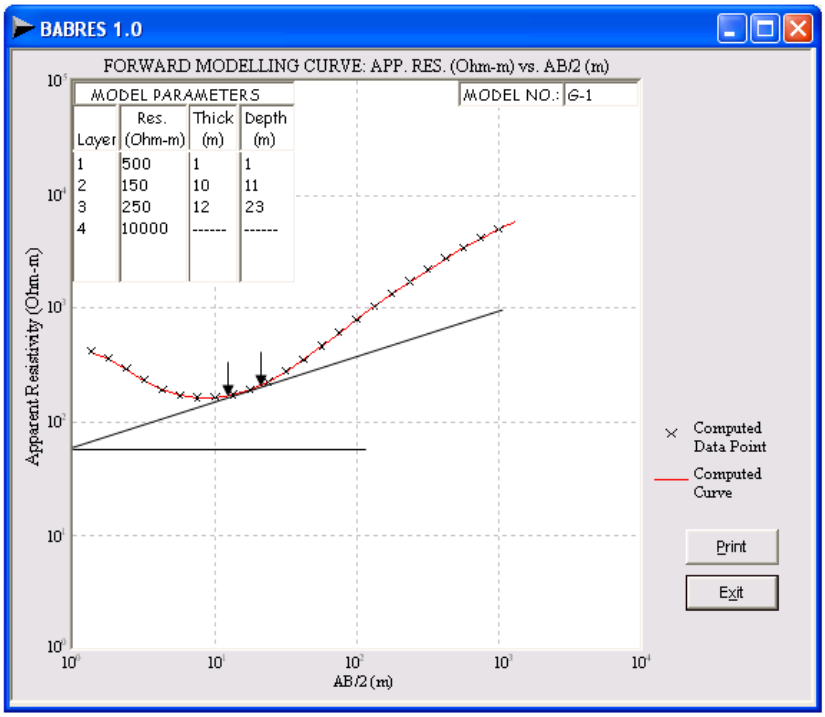

Zone detectable, drag length (dl)= 0.50cm, drag angle β = 20°

Figure 14: HA-Type Curve Model G1 for Resistivity of Transition Zone Equals 250 ohm-m.

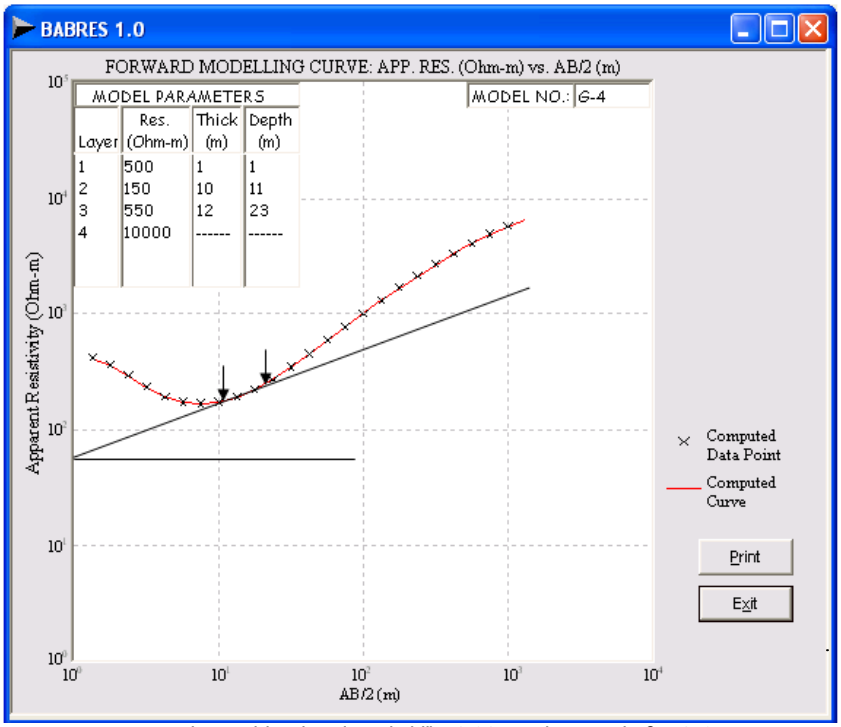

Zone detectable, drag length (dl)= 0.90cm, drag angle β = 21°

Figure 15: HA-Type Curve Model G4 for Resistivity of Transition Zone Equals 650 ohm-m.

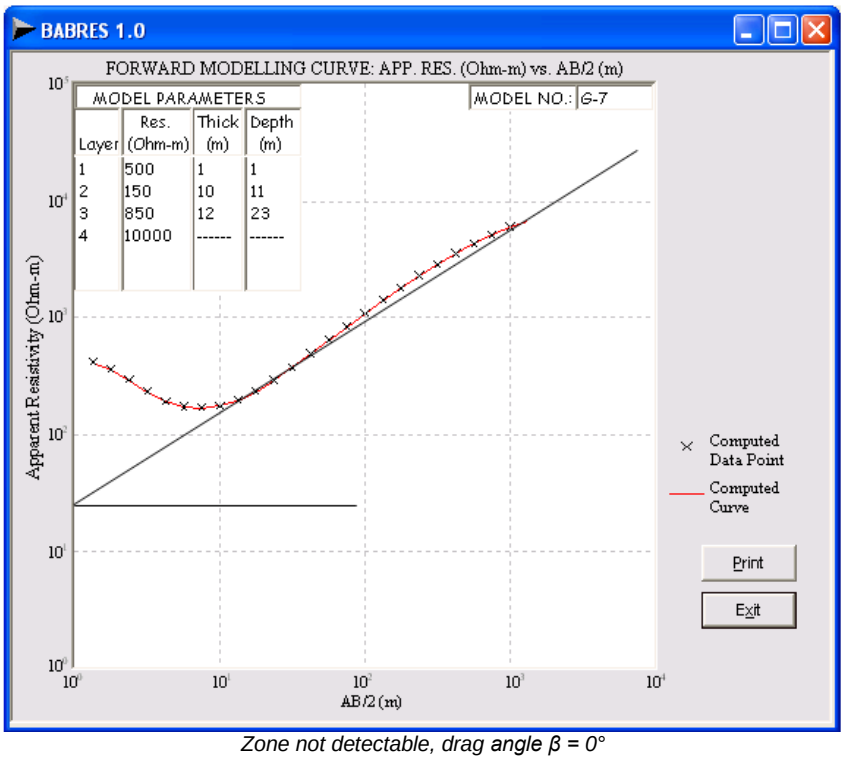

Zone not detectable, drag angle β = 0°

Figure 16: HA-Type Curve Model G7 for Resistivity of Transition Zone Equals 850 ohm-m.

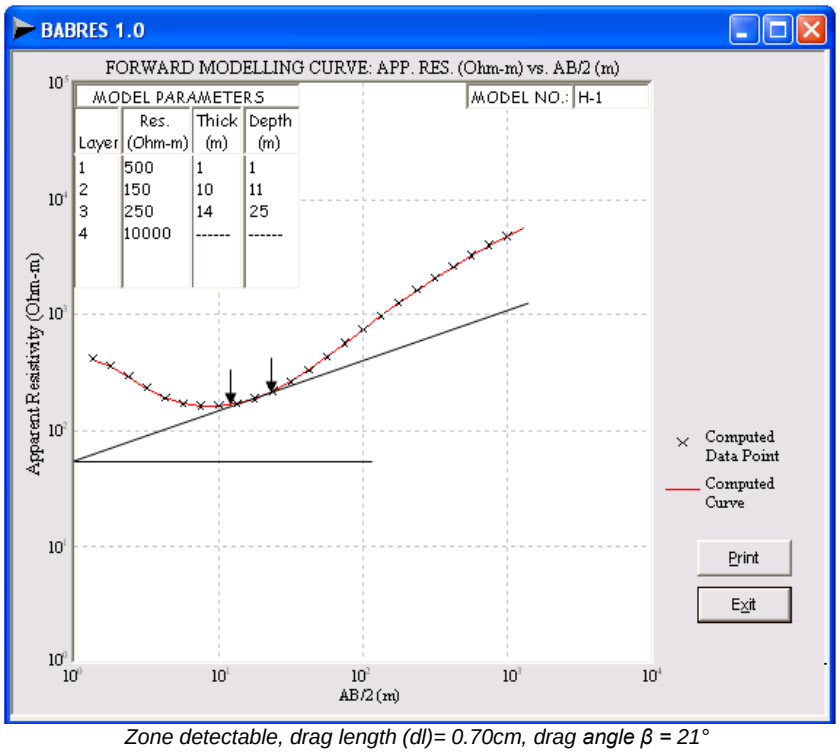

Zone detectable, drag length (dl)= 0.70cm, drag angle β = 21°

Figure 17: HA-Type Curve Model H1 for Resistivity of Transition Zone Equals 250 ohm-m.

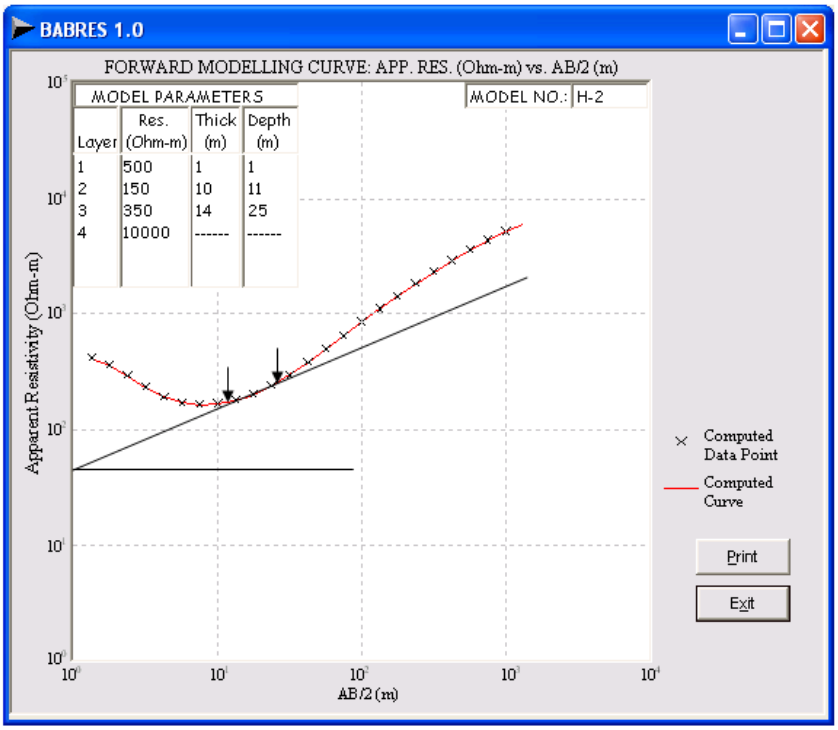

Zone detectable, drag length (dl)= 0.80cm, drag angle β = 22°

Figure 18: HA-Type Curve Model H2 for Resistivity of Transition Zone Equals 350 ohm-m.

Again, this procedure was repeated for the KHA-type curves except that the starting model has resistivity values of 200 ohm-m for topsoil layer, 750 ohm-m for the lateritic layer, 150 ohm-m for the weathered layer, 250 ohm-m for the transition zone and 10000 ohm-m for the fresh basement.

The thicknesses of the horizons are respectively fixed at 1m, 2.5m, and 10m for the three top layers, and 10m for the transition zone. As usual and again, each of the resulting parameter sets was used to generate seven (7) model curves numbered K1-K7, L1-L7, M1-M7, for the KHA-type curves (see Figures 19-25 for representative sample models generated for the KHA- type curve).

As in the first approach, the drag length was measured in curves where the zone is detectable, so also is the drag angle β^0. For each of the model curves allowing for detectability, the resistivity ratio of the transition zone to that of the overlying weathered layer (ρ_3/ρ_2) for the HA-, and ρ_4/ρ_3 for the KHA-type curves were calculated and recorded (see Tables 3 and 4 respectively for the summary of the resulting parameter sets and the obtained/measured specifications of the detectable transition zones for the HA- and KHA-type curves).

In the second approach and for the HA-type curves, the resistivities of the other three layers were fixed while that of the transition zone was varied. The resistivity was varied from 250 ohm-m to 850 ohm-m for the transition zone. For the starting model, the resistivities are 500 ohm-m for topsoil, 150 ohm-m for weathered layer, 250 ohm-m for the transition zone while the fresh basement has a resistivity of 10000 ohm-m.

The thicknesses of the starting models are 1 m for topsoil, 10 m for weathered layer while the transition zone has a thickness of 2 m. Each of the resulting parameter sets was used to generate seven (7) model curves numbered B1-B7, C1-C7, D1-D7, E1-E7, F1-F7, G1-G7,H1-H7 for the HA- type curves, (see Figures 12-18 for representative sample models generated for the HA- type curve).

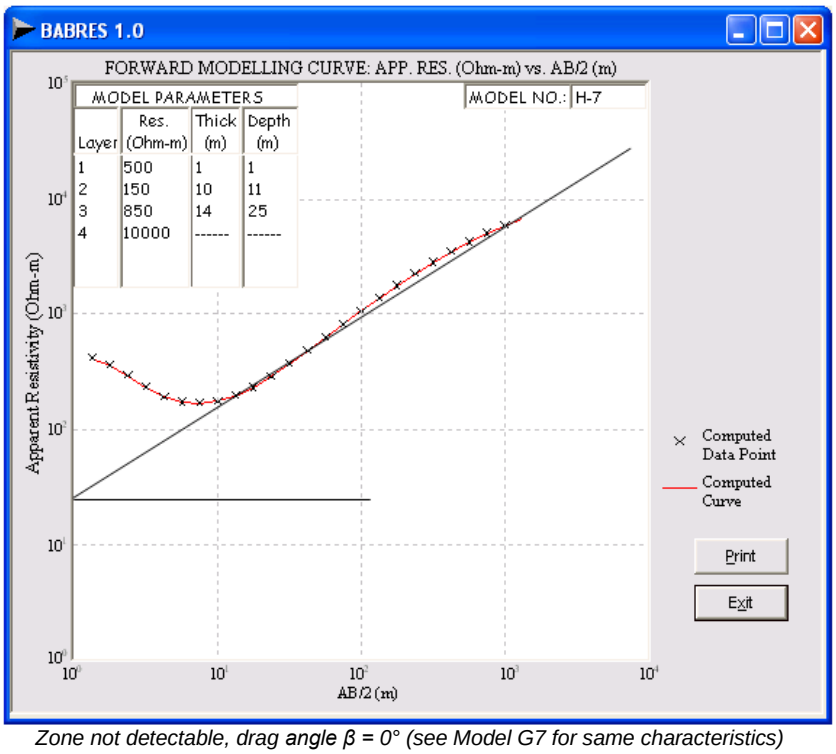

Zone not detectable, drag angle β = 0° (see Model G7 for same characteristics)

Figure 19: HA-Type Curve Model G7 for Resistivity of Transition Zone Equals 850 ohm-m.

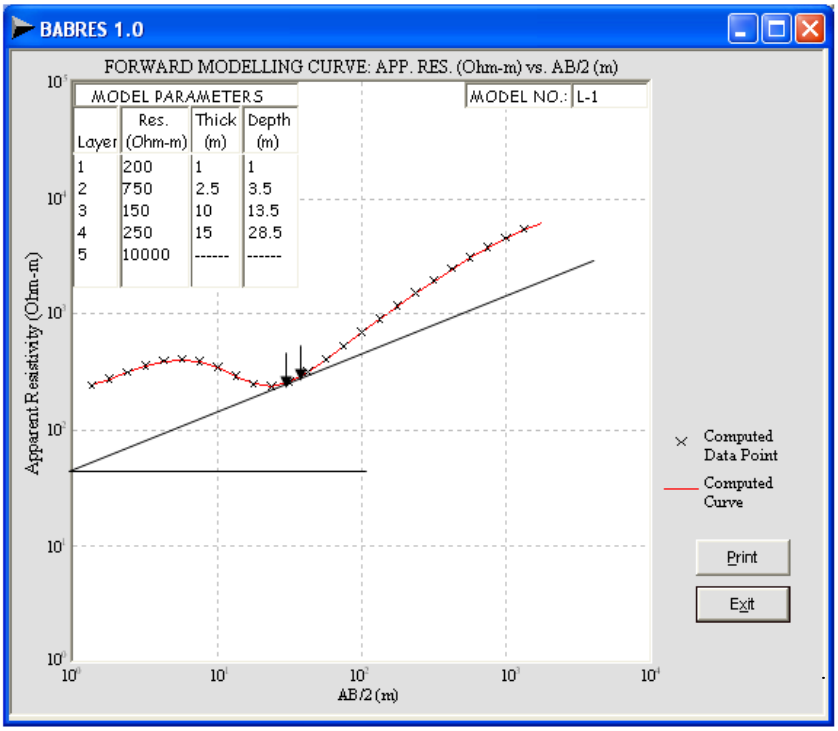

Zone detectable, drag length (dl)= 0.20cm, drag angle β = 21°

Figure 20: KHA-Type Curve Model L-1 for Resistivity of Transition Zone Equals 250 ohm-m.

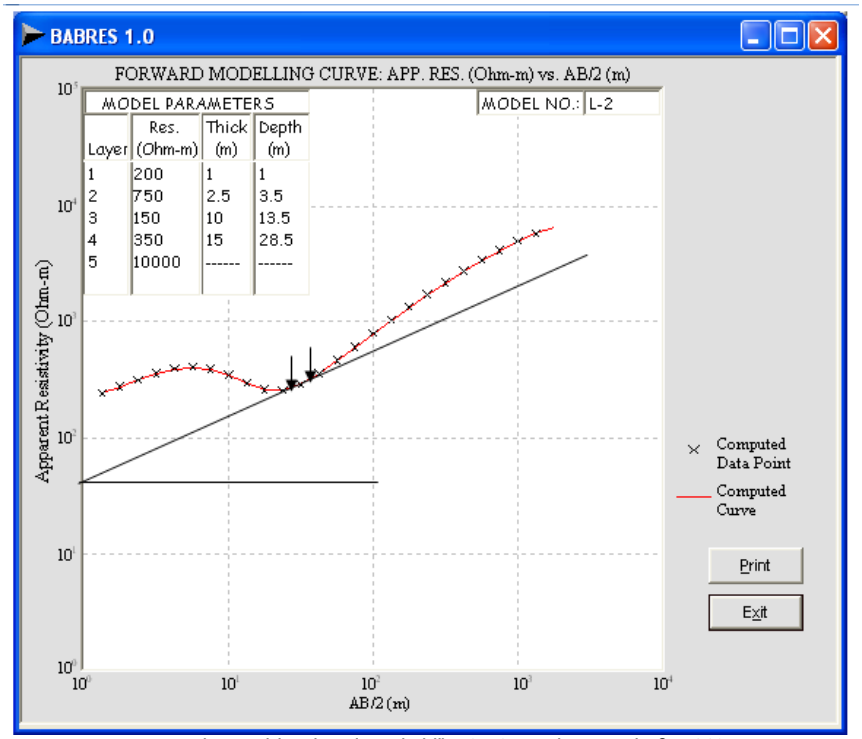

Zone detectable, drag length (dl)= 0.40cm, drag angle β = 23°

Figure 21: KHA-Type Curve Model L-2 for Resistivity of Transition Zone Equals 350 ohm-m.

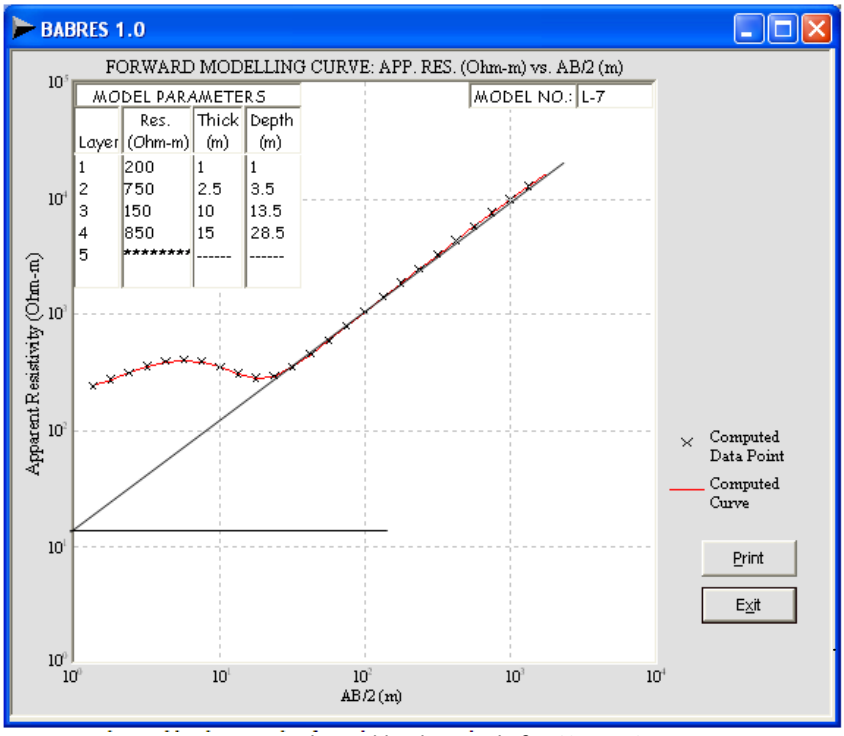

Zone not detectable, drag angle β = 0°, γ=41°

Figure 22: KHA-Type Curve Model L-7 for Resistivity of Transition Zone Equals 850 ohm-m.

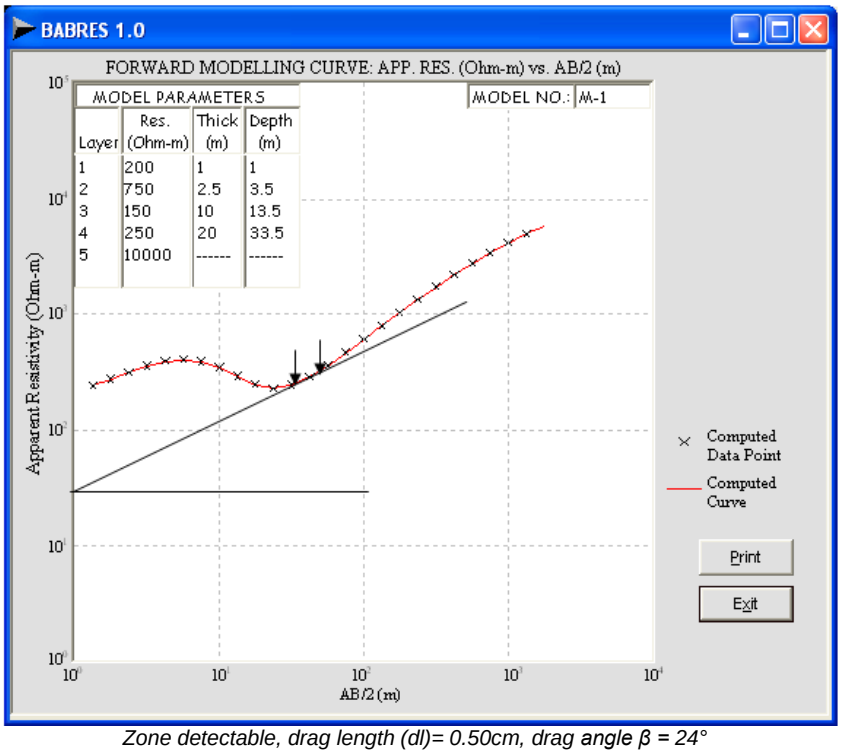

Zone detectable, drag length (dl)= 0.50cm, drag angle β = 24°

Figure 23: KHA-Type Curve Model M-1 for Resistivity of Transition Zone Equals 250 ohm-m.

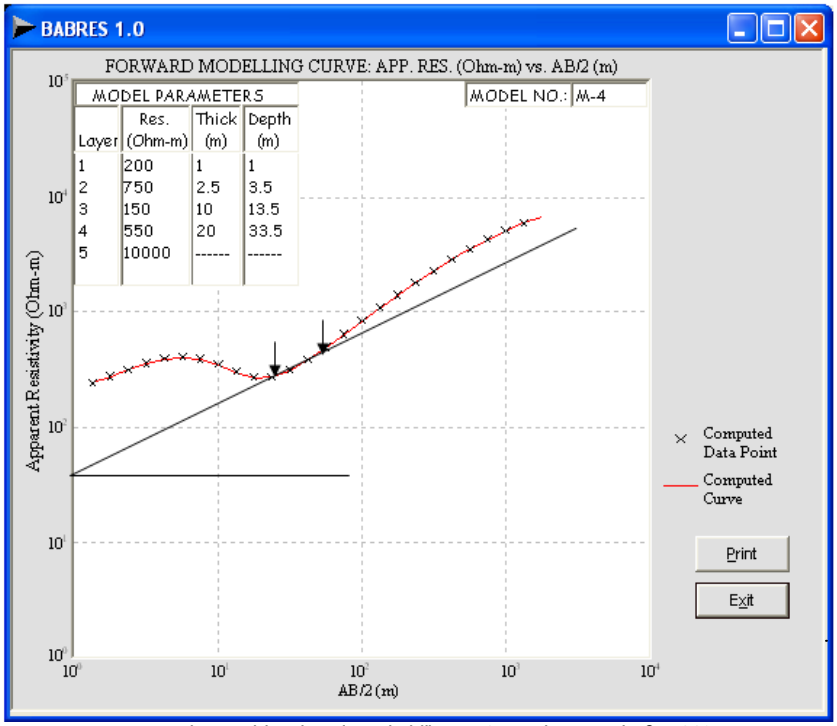

Zone detectable, drag length (dl)= 1.10cm, drag angle β = 22°

Figure 24: KHA-Type Curve Model M-4 for Resistivity of Transition Zone Equals 550 ohm-m.

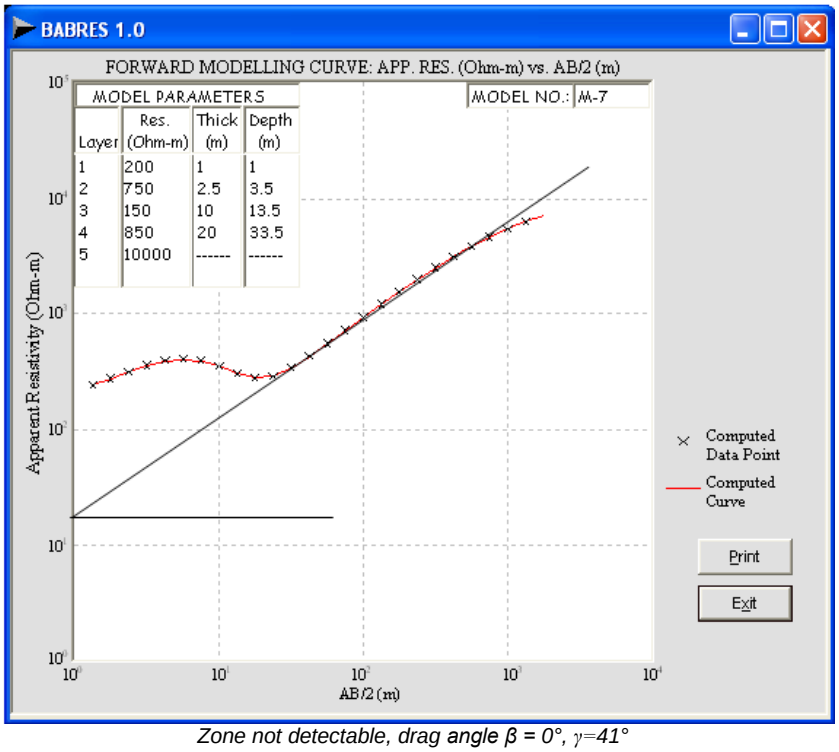

Zone not detectable, drag angle β = 0°, γ=41°

Figure 25: KHA-Type Curve Model M-7 for Resistivity of Transition Zone Equals 850 ohm-m.

Table 3A: Effect of Variation of Resistivity of Transition Zone on the Detectability Parameters of the HA-Type VES Curve.

Layer No	Thickness (m)	MODELS B1- B7 Resistivities (Ohm-m)						
1	1	500	500	500	500	500	500	500
2	10	150	150	150	150	150	150	150
3	2	250	350	450	550	650	750	850
4	-	10000	10000	10000	10000	10000	10000	10000
Remarks	TRANSITION ZONE NOT DETECTABLE							

Table 3B

Layer No	Thickness (m)	MODELS C1- C7 Resistivities (Ohm-m)						
1	1	500	500	500	500	500	500	500
2	10	150	150	150	150	150	150	150
3	4	250	350	450	550	650	750	850
4	-	10000	10000	10000	10000	10000	10000	10000
Remarks	TRANSITION ZONE NOT DETECTABLE							

Table 3C

Layer No	Thickness (m)	MODELS D1- D7 Resistivities (Ohm-m)						
1	1	500	500	500	500	500	500	500
2	10	150	150	150	150	150	150	150
3	6	250	350	450	550	650	750	850
4	-	10000	10000	10000	10000	10000	10000	10000
Remarks	TRANSITION ZONE NOT DETECTABLE							

Table 3D

Layer No	Thickness (m)	MODELS E1- E7 Resistivities (Ohm-m)						
1	1	500	500	500	500	500	500	500
2	10	150	150	150	150	150	150	150
3	8	250	350	450	550	650	750	850
4	-	10000	10000	10000	10000	10000	10000	10000
Remarks	TRANSITION ZONE NOT DETECTABLE							

Table 3E

Layer No	Thickness (m)	MODELS F1- F7 Resistivities (Ohm-m)						
1	1	500	500	500	500	500	500	500
2	10	150	150	150	150	150	150	150
3	10	250	350	450	550	650	750	850
4	-	10000	10000	10000	10000	10000	10000	10000
Remarks	TRANSITION ZONE NOT DETECTABLE							

Table 3F

Layer No	Thickness (m)	MODELS G1- G7 Resistivities (Ohm-m)						
1	1	500	500	500	500	500	500	500
2	10	150	150	150	150	150	150	150
3	12	250	350	450	550	650	750	850
4	-	10000	10000	10000	10000	10000	10000	10000
ρ_3/ρ_2		1.67	2.33	3.00	3.67	4.33	5.00	5.67
β^o		20	20	21	21	21	21	21
dL (cm)		0.50	0.55	0.70	0.90	0.50	0.40	0.00
Remarks		D	D	D	D	D	D	ND

Table 3G

Layer No	Thickness (m)	MODELS H1- H7 Resistivities (Ohm-m)						
1	1	500	500	500	500	500	500	500
2	10	150	150	150	150	150	150	150
3	14	250	350	450	550	650	750	850
4	-	10000	10000	10000	10000	10000	10000	10000
ρ_3/ρ_2		1.67	2.33	3.00	3.67	4.33	5.00	5.67
β^o		21	22	22	21	21	21	-
dL (cm)		0.70	0.80	0.95	0.70	0.60	0.40	0.00
Remarks		D	D	D	D	D	D	ND

Note : ND = Transition zone not Detectable , D = Transition zone detectable , dL = drag length , ρ_3 = Transition zone (3rd) layer resistivity, ρ_2 = weathered(2nd) layer resistivity, ρ_3/ρ_2 = Resistivity ratio

Table 4: Effect of Variation of Resistivity of Transition Zone on the Detectability Parameters of the KHA- type VES Curve.

LAYER NO	THICKNESS (M)	MODELS K1 – K7 RESISTIVITIES (OHM-M)						
1	1	200	200	200	200	200	200	200
2	2.5	750	750	750	750	750	750	750
3	10	150	150	150	150	150	150	150
4	10	250	350	450	550	650	750	850
5	-	10000	10000	10000	10000	10000	10000	10000
	P_4/ρ_3	1.67	2.33	3.00	3.67	4.33	5.00	5.67
	β^o	-	-	-	-	-	-	-
	dL (cm)	-	-	-	-	-	-	-
Remarks		ND	ND	ND	ND	ND	ND	ND

Table 4B

LAYER NO	THICKNESS (M)	MODELS L1 – L7 RESISTIVITIES (OHM-M)						
1	1	200	200	200	200	200	200	200
2	2.5	750	750	750	750	750	750	750
3	10	150	150	150	150	150	150	150
4	15	250	350	450	550	650	750	850
5	-	10000	10000	10000	10000	10000	10000	10000
	P_4/ρ_3	1.67	2.33	3.00	3.67	4.33	5.00	5.67
	β^o	21	23	24	23	22	21	-
	dL (cm)	0.30	0.40	0.70	0.50	0.30	0.20	-
Remarks		D	D	D	D	D	D	ND

Table 4C

LAYER NO	THICKNESS (M)	MODELS M1 – M7 RESISTIVITIES (OHM-M)						
1	1	200	200	200	200	200	200	200
2	2.5	750	750	750	750	750	750	750
3	10	150	150	150	150	150	150	150
4	20	250	350	450	550	650	750	850
5	-	10000	10000	10000	10000	10000	10000	10000
	P_4/ρ_3	1.67	2.33	3.00	3.67	4.33	5.00	5.67
	β^o	24	23	22	22	23	23	-
	dL (cm)	0.50	0.70	0.90	1.10	0.70	0.30	0,.00
Remarks		D	D	D	D	D	D	ND

Note : ND = Transition zone not Detectable , D = Transition zone detectable , dL = drag length , ρ_4 = Transition zone (4^{th}) layer resistivity, ρ_3 = weathered (3^{rd}) layer resistivity, ρ_4/ρ_3 = Resistivity ratio

Again, this procedure was repeated for the KHA-type curves except that the starting model has resistivity values of 200 ohm-m for topsoil layer, 750 ohm-m for the lateritic layer, 150 ohm-m for the weathered layer, 250 ohm-m for the transition zone and 10000 ohm-m for the fresh basement. The thicknesses of the horizons are respectively fixed at 1m, 2.5m, and 10m for the three top layers, and 10m for the transition zone. As usual and again, each of the resulting parameter sets was used to generate seven (7) model curves numbered K1-K7, L1-L7, M1-M7 for the KHA-type curves (see Figures 19-25 for representative sample models generated for the KHA- type curve).

As in the first approach, the drag length was measured in curves where the zone is detectable, so also is the drag angle β^0. For each of the model curves allowing for detectability, the resistivity ratio of the transition zone to that of the overlying weathered layer (ρ_3/ρ_2) for the HA-, and ρ_4/ρ_3 for the KHA-type curves were calculated and recorded (see Tables 3 and 4, respectively, for the summary of the resulting parameter sets and the obtained/measured specifications of the detectable transition zones for the HA- and KHA-type curves).

RESULTS AND DISCUSSION

Arising from the study and analysis of these generated models, the following questions arise, answers to which would facilitate a focused discussion and subsequent understanding of the obtained results:

(i.) At what thickness ratio does the transition zone becomes detectable on the VES curve?

(ii.) What are the resistivity ratios and resistivity reflection coefficients allowing for the detectability of the transition zone? and

(iii.) How do the thickness and resistivity ratios impact on the drag length?

Considering the first set of models generated using the developed software, detailed summary of parameters of which are presented in Tables 1 and 2 , it could be observed that the transition zone is not detectable for thickness ratios below 0.73 for the HA-type, and 1.11 for the five-layer KHA-type curves. At these ratios, the zone debuts with a drag length of 0.3 cm and 0.2 cm, respectively, on the HA- and the KHA-type curves. This is in agreement with Olayinka and Oladipo (1994), when they posited that, "for a layer to be detectable, its thickness does not necessarily have to be larger than its depth of burial; rather it could just be a fraction of the depth of burial" and Zohdy, et al., (1974) which observed that the minimum relative thickness permitting for detectability can vary from less than 0.5 to well over 1.0.

From Tables 1 and 2 it could be observed that the effect of marginal increase in the thickness ratio does not readily impact noticeably on the drag length. Only a substantial increase would result in observable increase. Figures 26 and 27 show that the drag length increases polynomially with the thickness ratio. Therefore, it is reasonable from the evidences seen, to infer that an increase in the thickness ratio leads to an increase in drag length. Another inference from this is that, above the minimum detectable thickness ratio, the zone would continue to be recognized on the VES curve for the same range of resistivity ratio. From Tables 3 and 4, it is shown that the transition zone could not be detected below resistivity ratio of 1.67 for both curve types, and beyond 4.33 and 5.00 for HA and KHA type curves, respectively.

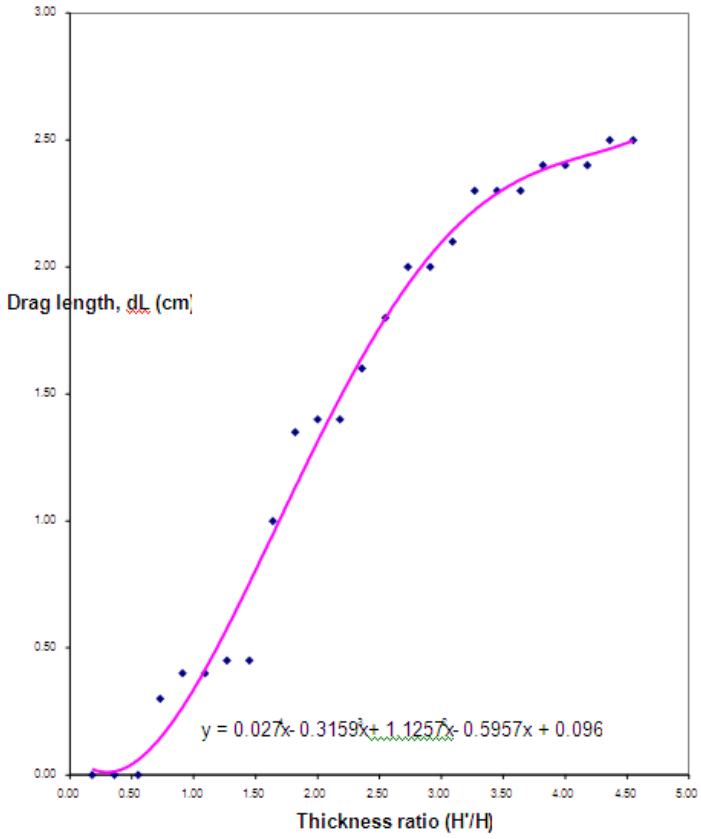

Figure 26: Graph of Drag Length against Thickness Ratio for HA-Type Curve.

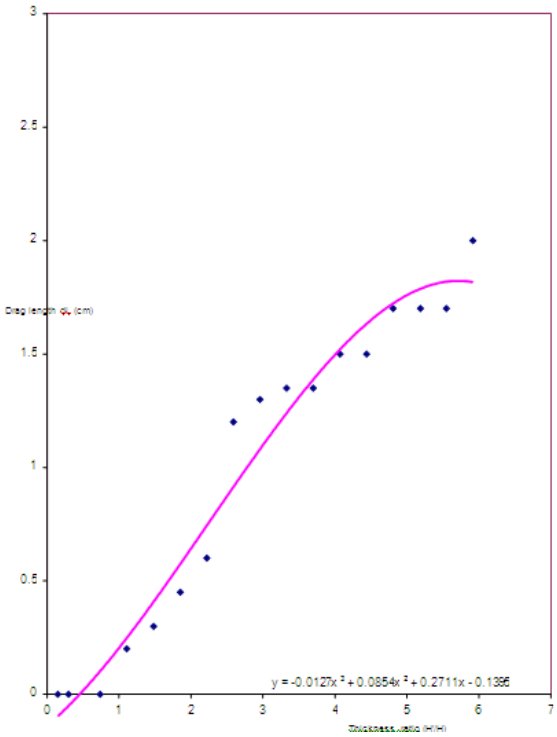

Figure 27: Graph of Drag Length against Thickness Ratio for KHA-Type Curve.

The drag length steadily increases with increase in resistivity ratio up to an optimum value between 3.0 and 3.67 for HA-type curve and 3.80 and 4.50 for the KHA-type curve, and subsequently decrease with increase in the resistivity ratios (see Figures 28 and 29).

At these optimum values, the drag length reaches its maximum and the zone becomes mostly pronounced and easily detectable on the VES curves. An increase beyond the upper limit in resistivity ratio would lead to a decrease in drag length and finally leads to undetectability of the zone on the VES curve because, the resistivity reflection coefficient (k) between the transition zone and the underlying fresh bedrock approaches +1, which makes differentiation of the zone from the fresh bedrock difficult .However, it must be stated that, for the zone to be detectable within the resistivity ratio ranges stated above, the corresponding thickness ratios (TR1 or H'/H) must not fall below the limits specified earlier (i.e., 0.73 for the HA- and 1.10 for the KHA- type curves).

The inferences from these is that while the thickness ratio is independent of the resistivity ratio within the specified limits, the reverse is the case for the resistivity ratio limits as they are valid only for corresponding values of thickness ratios not below the minimum limits (i.e., 0.73 for HA-, and 1.10 for KHA-type curves). From the foregoing, it could therefore be concluded that the transition zone can be identified on the VES curve when the ratio of the thickness of the zone to that of the overlying layers is not less than 0.73 for the HA- and 1.11 for the KHA-type curves. Also the resistivity ratio of the zone to that of the immediately overlying weathered layer must range from 1.67 to 4.33 for the HA- and 1.67 to 5.00 for the KHA-type curves.

Above these ranges, the zone becomes difficult to differentiate from the fresh basement. Also, while the resistivity ratio limits depend on the minimum thickness ratio requirements for its validity, the thickness ratio is valid for all resistivity ratios. However, for optimum detectability, the resistivity ratio should be between 3.0 and 3.67 for the HA-type curve and 3.8 – 4.50 for the KHA-type curve.

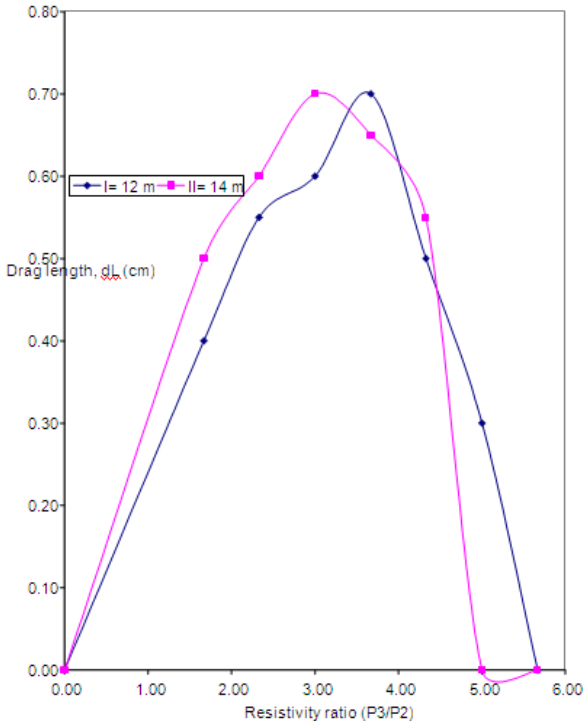

Figure 28: Graph of Drag Length against Resistivity Ratio for HA-Type Curve.

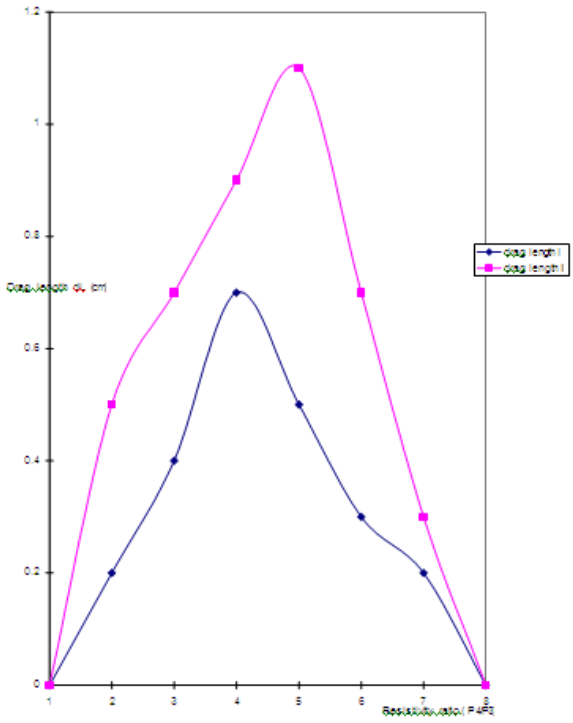

Figure 29: Graph of Drag Length against Resistivity Ratio for HA-Type Curve.

CONCLUSION AND RECOMMENDATION

The transition zone manifests as a drag along the rising segment of an HA-curve or curves ending with HA-. Where this drag is noticeable, the curve is correctly interpreted as a four-layer HA-type curve. However, where the reverse is the case and in which case, the drag becomes undetectable, the curve is inadvertently and incorrectly interpreted as a three-layer H-type curve, or in the case of the five-layer KHA-, as a four-layer KH- type curve, thus resulting in a serious interpretation problem, since subsequent actions supposedly on the interpretation would be based on this faulty premise. The rocks of the basement complex of Southwest Nigeria constitute the regional geology of the area under study.

The research approach adopted has been to use a forward modeling computer software BABRES 1.0 developed by the authors for this purpose to generate theoretical Schlumberger Vertical Electrical Sounding (VES) curves in order to theoretically model the basement profile containing a transition zone (saprock) with varying thicknesses and resistivities as a means of assessing the detectability of the hydrogeologically important zone with often small thickness.

The software was used to generate series of four-layer HA-type and five-layer KHA-type model curves with varying thicknesses and resistivities. For the HA-type curve, keeping the resistivities constant at 500 ohm-m, 150 ohm-m, 300 ohm-m and 10000 ohm-m respectively for the topsoil, weathered layer, transition zone and fresh bedrock, and the thicknesses of 1 m for topsoil, and 10 m for weathered layer, the thickness of the transition zone was varied between 2 m and 50 m.

For the KHA-type model curve, the resistivites were kept constant at 200 ohm-m for the topsoil, 750 ohm-m for the lateritic layer,150 ohm-m for the weathered layer, 250 ohm-m for the transition zone and 10000 ohm-m for the fresh bedrock, while the thicknesses were fixed at 1m, 2.5m, and10m for the three top layers. The thickness of the transition zone was varied between 5m and 80m.

The resulting model parameters for each variation was used to generate a model curve depicting each situation (Figures 3–11 for representative sample models) and each curve was examined carefully for signatures of the transition zone in terms of the drag length in order to resolve the detectability problem. From this, it was discovered that the transition zone becomes detectable when the ratio of the thickness of the transition zone to that of the overburden is greater than or equal to 0.73 for the HA-type and 1.11 for the KHA-type curve. Again, keeping the thicknesses constant at 1 m, 10 m and 2m respectively for the topsoil, weathered basement and transition zone while fixing the resistivities of the topsoil and weathered basement at 500 ohm-m and 150 ohm-m, respectively, the resistivity of the transition zone was varied from 250 ohm-m to 850 ohm-m to generate HA-type model curves. This procedure was also repeated for the KHA-type except that the thicknesses were fixed at 1m, 2.5m, and 10m, respectively, for the topsoil, lateritic layer, weathered basement, and transition zone while fixing the resistivities of the topsoil, lateritic layer, and weathered layers at 200 ohm-m,750 ohm-m, and 150 ohm-m, respectively.

The resistivity of the transition zone was also varied from 250 ohm-m to 850 ohm-m for the generation of the KHA-type model curves. For these fixed thickness and resistivity range, the transition zone was not detectable from the generated model curves of both HA- and KHA-types (see Figures 12- 18 for representative sample models).

Furthermore, the values of the thicknesses of the transition zone were thereafter varied in steps of 2m (i.e., 4m, 6m, 8m,10m,12m, etc.) for the HA-type models and 5m (i.e., 15m, 20m, 25m, 30m, etc.) for the KHA-type models with the previous parameters of the other horizons unchanged. The procedure was repeated for the generation of more model curves of both types from which the transition zone now becomes detectable (Figures 19-25).

From the above, it was discovered that the resistivity ratio permitting detectability of the zone was discovered to range from 1.67 to 4.33 for the HA-type curve and 1.67 to 5.00 for the KHA-type curve, while for optimum detectability , the ratio should be between 3.0 and 3.67 for HA-type and 3.8 – 4.50 for the KHA-type curve. Beyond these ranges of resistivity ratios, the transition zone becomes undetectable. The drag length was observed to increase with the thickness ratio and furthermore, it was discovered that while the thickness ratio is independent of the resistivity

ratio within the specified limits, the reverse is the case for the resistivity ratio limits, as its validity depends on keeping the corresponding thickness ratio at minimum values (i.e., 0.73 for HA- and 1.10 for KHA- type curves).

RECOMMENDATIONS

Arising from the results and conclusions of this research work, it is should be noted that even though the curve types and the generated models used for this work could be said to be of relatively large numbers, it is still conceded that the theoretical models considered in this study are by no means exhaustive, being limited to the HA- and the KHA- type models. Therefore it is recommended that future work be extended to other multi-layered earth models with type curves ending with HA- in order to further confirm the results from this study.

REFERENCES

1. Ademilua, O. L. 2007. "Computer Modelling and Detectability Assessment of the Transition Zone in the Basement Complex Terrain of Southwest Nigeria". Unpublished Ph.D. Thesis. Dept. of Geology, Obafemi Awolowo University: Ile-Ife, Nigeria. 438.

2. Ademilua, O.L. and Olorunfemi, M.O. 2007. "An Interactive Software for Schlumberger Theoretical Resistivity Forward Modelling". *Journal of Applied and Environmental Sciences.* Louisville, KY. 3(2):96-107.

3. Acworth, R.I. 1987. "The Development of Crystalline Basement Aquifers in Tropical Environment". *Quarterly Journal of Engineering Geology*. 20:265-272.

4. Barker, R.D. 1992. "A Simple Algorithm for Subsurface Imaging". *First Break*. 10:53-62.

5. Beeson, S. and Jones, C.R.C. 1988. "The Combined EMT/VES Geophysical Method for Siting Boreholes". *Groundwater*. 26(1):54-63.

6. Buckley, D.K. and Zeil, P. 1984. "The Character of Fractured Rock Aquifer in Eastern Botswana". *IAHS publication*. No 144:25-36.

7. Caruthers, R.M. and Smith, I.F. 1992. "The use of Ground Electrical Survey Methods for Siting Water Supply Boreholes in Shallow Crystalline Basement Terrains". In: Wright, E.P. and Burges, W. G. (eds). *The Hydrogeology of Crystalline Basement Aquifers in Africa*. Geological Society Special Publications. No 66:2203-2208.

8. David, L.M. Jr. 1988. "Geoelectrical Study of Shallow Hydrogeological Parameters in the area around Idanre, Southwestern Nigeria. Unpublished Ph.D. Thesis. University of Ibadan, Ibadan, Nigeria.

9. Flathe, H. 1963. "Five-Layer Master Curves for the Hydrogeological Interpretation of Geoelectric Resistivity Measurements above a Two-Story Aquifer". *Geophysical Prospecting*. 11:471-508.

10. Hazel, J.R.T., Cratchley, C.H., and Preston, A.M. 1988. "The Location of Aquifers in Crystalline Rocks and Alluvium in Northern Nigeria with Resistivity Techniques". *Quarterly Journal of Engineering Geology*. 21:159-175.

11. Irshad, R.M. 1976. "Finite-Difference Resistivity Modelling for Arbitrarily Shaped Two-Dimensional Structures. *Geophysics*. 41(1):62-78.

12. Kunetz, G. 1966. *Principles of Direct Current Resistivity Prospecting*. Borntrager: Berlin, Germany. 106.

13. Mailet, R. 1947. "The Fundamental Equations of Electrical Prospecting. *Geophysics*. 12:529-556.

14. Mooney, H.M., Orellana, E., Pickett, H. and Iornheim, L. 1966. "A Resistivity Computation Method for Layered Earth Models". *Geophysics*. 3:199-203.

15. Olayinka, A.I. 1996. "Non-Uniqueness in the Interpretation of Bedrock Resistivity from Sounding Curves and its Hydrogeological Implications. *Journal of Nigerian Association of Hydrogeologists*. 7(1 & 2):49-55.

16. Olayinka, A.I. and Oladipo, A.O. 1994. "A Quantitative Assessment of Geoelectrical Suppression in Four-Layer HA-type Earth Model". Journal ff Min. and Geology. 30(2):251-258.

17. Olorunfemi, M.O., Fatoba, J.O., and Ademilua, L.O. 2005. "Integrated VLF-Electromagnetic and Electrical Resistivity Survey for Groundwater in a Crystalline Basement Complex Terrain of Southwest Nigeria". *Global Journal of Geological Sciences*. 3(1):71-80.

18. Parasnis, D.S. 1986. *Principles of Applied Geophysics. 4th Ed*. J.W. Arrosmit, Ltd.: Brisol, UK.

19. Parasnis, D.S. 1994. *Principles of Applied Geophysics*. J. W. Arrowsmith Ltd.: Bristol, UK. 102-169.

20. Verma, R.K., Rao, M.K., and Rao, C.V. 1980. "Resistivity Investigations for Groundwater in Metamorphic Areas Near Dhanbad, India". *Groundwater*. 18:46-55.

21. White, C.C., Houston, J.F.T., and Barker, R.D. 1988. "The Victoria Province Drought Relief Project I. Geophysical Siting of Borehole". *Groundwater*. 26:309-316..

22. Zohdy, A.A.R., Easton, G.P., and Mabey, D.R. 1974. "Application of Surface Geophysics to Groundwater Investigations". *U.S. Geological Survey Techniques of Water Resources Investigations*. Book 2, Chapter D1.

ABOUT THE AUTHORS

Ademilua Oladimeji Lawrence received his M.Sc. and Ph.D. in Applied Geophysics from the Obafemi Awolowo University, Ile–Ife Nigeria, and he is currently a Lecturer Grade 1 at the Geology Department of the University of Ado Ekiti,, Nigeria.

Olorunfemi Martins Olu received his B.Sc., M.Sc., and Ph.D. in Applied Geophysics from the University of Birmingham, U.K., and he has edited several journals at both local and international levels. He is currently a Professor of Applied Geophysics at the Geology Department of the Obafemi Awolowo, University Ile-Ife, Nigeria.

SUGGESTED CITATION

Ademilua, L.O. and M.O. Olorunfemi. 2010. "Computer Modeling for Assessing the Detectability of the Transition Zone in the Basement Complex Terrain of Southwest Nigeria". *Pacific Journal of Science and Technology*. 11(2):674-698.